ELSEVIER

Contents lists available at ScienceDirect

Earth and Planetary Science Letters

journal homepage: www.elsevier.com/locate/epsl



Check for updates

Bayesian frameworks for integrating petrologic and geochronologic data

Ian W. Hillenbrand*, Michael L. Williams

Department of Earth, Geographic, and Climate Sciences, University of Massachusetts Amherst, Amherst, MA 01003, USA

ARTICLE INFO

Editor: Dr A Webb

Keywords:
Bayesian statistics
Age-sequence modeling
Change point analysis
Petrochronology
Monazite
Reaction dating

ABSTRACT

Constraining the absolute time and duration of geologic processes is one of the great challenges and goals in Earth sciences. Increasingly, the integration of geochronologic constraints with petrologic information is being qualitatively applied to understanding the timescales of metamorphic, igneous, tectonic, and fluid-related processes. Many rocks and geochronometers preserve relative age constraints such as compositional zoning or cross cutting relationships. This prior information can be formalized in a Bayesian statistical framework to generate a probabilistic posterior chronology. As we show here, these "age-sequence" models can enhance precision on geochronologic dates and rates and insight into tectonic models. Bayesian modeling of complex, concentrically, zoned monazite from the northern Appalachian orogen was used to develop a detailed temperature-time history through the Acadian (~405-395 Ma) and Neoacadian (~380-350 Ma) orogenies with significantly reduced uncertainties (40-70 %). Modeling of zoned monazite from a southern Trans-Hudson orogen granulite yielded durations of $0.5^{+9}/_{-0.4}$ Ma and $20^{+5}/_{-8}$ Ma for biotite-dehydration melting and suprasolidus conditions, respectively. The relatively short intervals of heating and peak conditions are consistent with a back-arc tectonic setting. A complementary approach, Bayesian change point detection, provides a framework to constrain the timing of compositional changes that can be linked with metamorphic reactions. Applying this approach in the northern Appalachian orogen demonstrates contrasting durations of low-Y monazite crystallization (~10 vs ~30 myr) in regions with different pressure-temperature histories. Compositionally distinct monazite domains can be linked with garnet stability, which provides a key constraint on tectonic models. Bayesian statistical analysis represent a powerful tool that can be widely applied to refine the absolute time and duration of geologic processes. A more objective and reproducible set of interpretations are produced by this more formal, although not necessarily complex, statistical analysis.

1. Introduction

A key goal in Earth science is to utilize mineral compositions and mineral reactions to constrain the timescales and rates of metamorphic, igneous, tectonic, and fluid-related processes (Baxter et al., 2017; Dumond et al., 2008; Foster et al., 2000). Over the last 20 years, developments in *in-situ* analytical methods have permitted the analysis of smaller volumes and the simultaneous acquisition of paired geochemical and geochronologic data (Engi, 2017; Kylander-Clark et al., 2013; Williams et al., 2017). However, key challenges remain in the interpretation of geochronologic data. Relatively short-lived processes and events can be challenging to differentiate within the uncertainty of *in-situ* analytical techniques (~1–2 %; Kylander-Clark et al., 2013). Also, protracted mineral growth may lead to a spread in measured dates in excess of analytical uncertainty (Klein and Eddy, 2023). The range in dates may make it challenging to evaluate the precise points at which mineral

compositions change, particularly in a quantitative and systematic manner

Many rocks and minerals preserve compositional or textural (relative) age constraints that can be incorporated with radiometric dates to yield a more precise understanding of the geologic history. In particular, compositional zoning in minerals such as monazite, xenotime, zircon, titanite, and garnet, and reaction textures among chronometer minerals are important relative timing constraints. That is, a statistically-based model can be developed for the tectonic history of a rock similar to age-depth modeling that is widely applied in the radiocarbon community (Haslett and Parnell, 2008) and, more recently, has been extended to deep-time stratigraphic applications (Johnstone et al., 2019; Pye et al., 2022; Trayler et al., 2019; Farrell et al., 2024). Bayesian statistical analysis provides the formalism to integrate relative timing constraints (priors) with geochronologic data (likelihoods) (Trayler et al., 2019, 2024; van de Schoot et al., 2021; Farrell et al., 2024).

E-mail address: ihillenbrand@umass.edu (I.W. Hillenbrand).

^{*} Corresponding author.

In this contribution, we demonstrate the utility and added insight of applying Bayesian statistical methods to petrochronologic data. First, we leverage relative timing constraints to improve the precision of geochronologic dates and rates in zoned minerals (age-sequence modeling). Second, we utilize a complementary Bayesian approach, step change analysis, to develop a quantitative framework to interpret time series data. The examples highlight how Bayesian analysis combining textural and geochronologic data can provide a better understanding of metamorphic heating and cooling rates and the duration of metamorphic events, which in turn yield new and tighter constraints on tectonic models. Overall, application of a more formal, although not necessarily complex, Bayesian statistical analysis to petrochronological data may provide a more objective and reproducible set of interpretations compared to visual inspection alone.

2. Methods

In this contribution we focus on monazite (LREEPO₄) and to a lesser extent on xenotime (YPO₄). These phases have been viewed as "ideal" for petrochronology due to their wide stability field in pressure-temperature-composition (P-T-X) space, broad compositional range that facilitates interaction in a variety of silicate reactions, high concentrations of U and Th, minimal common Pb, and high closure temperatures (>800 °C) (Engi, 2017; Kylander-Clark et al., 2013; Spear and Pyle, 2002; Williams et al., 2017). We applied Bayesian statistical analysis to monazite and xenotime data from recent petrochronologic studies (Hillenbrand et al., 2023a, 2023b, 2024a). Salient aspects of the analytical methods in these studies are summarized below; readers are referred to the original publications for detailed descriptions of the samples, datasets, and the analytical methods.

2.1. Petrochronology

Compositional maps of Mg, Ca, Ce, and Y were collected for entire polished thin sections using the Cameca SX100 at the University of Massachusetts to identify all major phases and locate all monazite and xenotime crystals in microstructural context. High resolution (0.5-to-1.0-micrometer step size) maps of Y, Th, U, Ca in monazite and Yb, Dy, Gd, and U in xenotime were collected for 25 to 40 grains per thin section. Grains maps were simultaneously processed using Adobe Photoshop CC to compare relative intensities and zoning characteristics across grains (Williams et al., 2017, 2007). These maps were used to develop an analytical strategy with the goal of analyzing each domain type, defined here as a compositionally homogenous region in one or more grains. Each domain type was analyzed (dated) multiple typically three or more, times. Preference was given to grains with multiple compositional domains to leverage their relative age constraints. Monazite and xenotime were analyzed for major- and trace-element compositions, and U-Th-Pbtotal dating using the Cameca Ultrachron at the University of Massachusetts (methods of Williams et al., 2017 and Hillenbrand et al., 2023a and references therein;). Each compositional domain was sampled with a single background analysis utilizing the multi-point method (Allaz et al., 2019) followed by 3 to 7 "peak" measurements. Uncertainty was calculated via propagation of the measurement and background errors through the "age equation" following Williams et al. (2017, 2007).

2.2. Trace element thermometry

Direct temperature-time constraints utilized the Y-based monazite-xenotime (Heinrich et al., 1997), monazite-garnet (Hacker et al., 2019), and xenotime-garnet (Pyle and Spear, 2000) thermometers where appropriate. Equilibrium between monazite, xenotime, and garnet equilibrium was assessed using the criteria of Pyle et al. (2001) and Hillenbrand et al. (2023a). In general, monazite and xenotime pairs were selected (1) that are located in the same microstructural domain

and (2) that yield statistically indistinguishable dates. Monazite-garnet and xenotime-garnet thermometry involved pairing monazite and xenotime crystals entirely enclosed by the garnet porphyroblast and which did not intersect fractures in the associated garnet domain. Errors for trace element thermometers have been estimated at $\sim 50~^{\circ}$ C (Daniel and Pyle, 2006; Hacker et al., 2019; Heinrich et al., 1997; Pyle and Spear, 2000).

2.3. Bayesian age-sequence modeling

Bayesian 'age-sequence' analysis was carried out using the "Ages of Stacked Beds" utility in Isoplot 4.0 (Ludwig, 2003). This Bayesian statistical tool uses a Monte Carlo approach and is applicable to cases where a clear relative age progression is observed. This tool was originally intended for stratigraphic analysis but is applicable to a broader range of scenarios as described in this contribution. The models in this study were conditioned with the combination of the obtained U-Th-Pb_{total} dates for each compositional domain (likelihood) and the prior that the age must decrease following the observed zoning patterns and textural relationships. Paths that violated this geometric constraint were rejected. The models were run a minimum of 10,000 times. Steps to carry out this analysis are as follows:

- Identify a relative age progression from geologic and/or petrologic observations.
- 2. Enter the ages and their uncertainties in an Excel worksheet The values should be ordered with the relatively oldest values at the bottom and youngest at the top.
- 3. Open the Ages of Stacked Beds utility. Select the relevant data and access the Ages of Stacked Beds utility via the Stacked Beds button of the Isoplot Charts & Isochrons toolbar or select Ages of Stacked Beds from the Isochron or Plot Type drop-down menu.
- 4. Verify the ages and errors in the resulting dialog box, and specify the type and sigma-level of the uncertainties. Specify the number of trials, noting that fewer trials will yield faster results while more trials will have better accuracy. Selecting the construct option will graph the probability distributions for the ages themselves or their differences. Selecting "go" will run the utility.

2.4. Bayesian change point analysis

Change point analysis identifies instances where the probability distribution of a time series changes (Page, 1954). We carried out change point analysis using the R-based package mcp (Lindeløv, 2020), which uses a Bayesian Markov Chain-Monte Carlo (MCMC) approach for univariate regression analysis. This package aims to provide maximum flexibility for analyses with *a priori* knowledge about the number of change points and the form of the intervening segments (Lindeløv, 2020). Here, we describe the application of this method to petrochronologic data.

- Import petrochronologic data. Datasets analyzed in mcp need dates and one or more compositional parameters.
- 2. Select the number of change points. The number of change points for which the model searched was manually specified based on the number of inferred change points, in this case the number of compositional domains. For example, a sample with three compositional domains would have two change points, one corresponding to each compositional change. We note that other change point algorithms can automatically infer change points, our focus here is on the insights gained from pairing petrologic observations with statistical models.
- 3. Run MCMC model. Calculations in R used an initial 5000 runs as a burn in followed by 10,000 iterations using three virtual cores operating in parallel to reduce computational time.

4. Assess convergence. The convergence of MCMC simulations can be assessed using Gelman and Rubin's convergence diagnostic (Rhat). This metric compares the between- and within-chain estimates for the model parameters. By using multiple chains and comparing within-chain and between-chain variances, the Gelman-Rubin diagnostic helps ensure that the MCMC simulation has sufficiently explored the parameter space and provides reliable estimates of the posterior distribution. If Rhat is close to 1 (typically below 1.1), it suggests that the chains have converged. This indicates that the

within-chain variance and the between-chain variances are similar. Values significantly greater than one indicates that the chains have not yet converged, and more iterations or a different number of change points might be needed.

3. Results and applications

We present several case studies in which we utilized Bayesian modeling in order to refine the timescales of metamorphic and tectonic

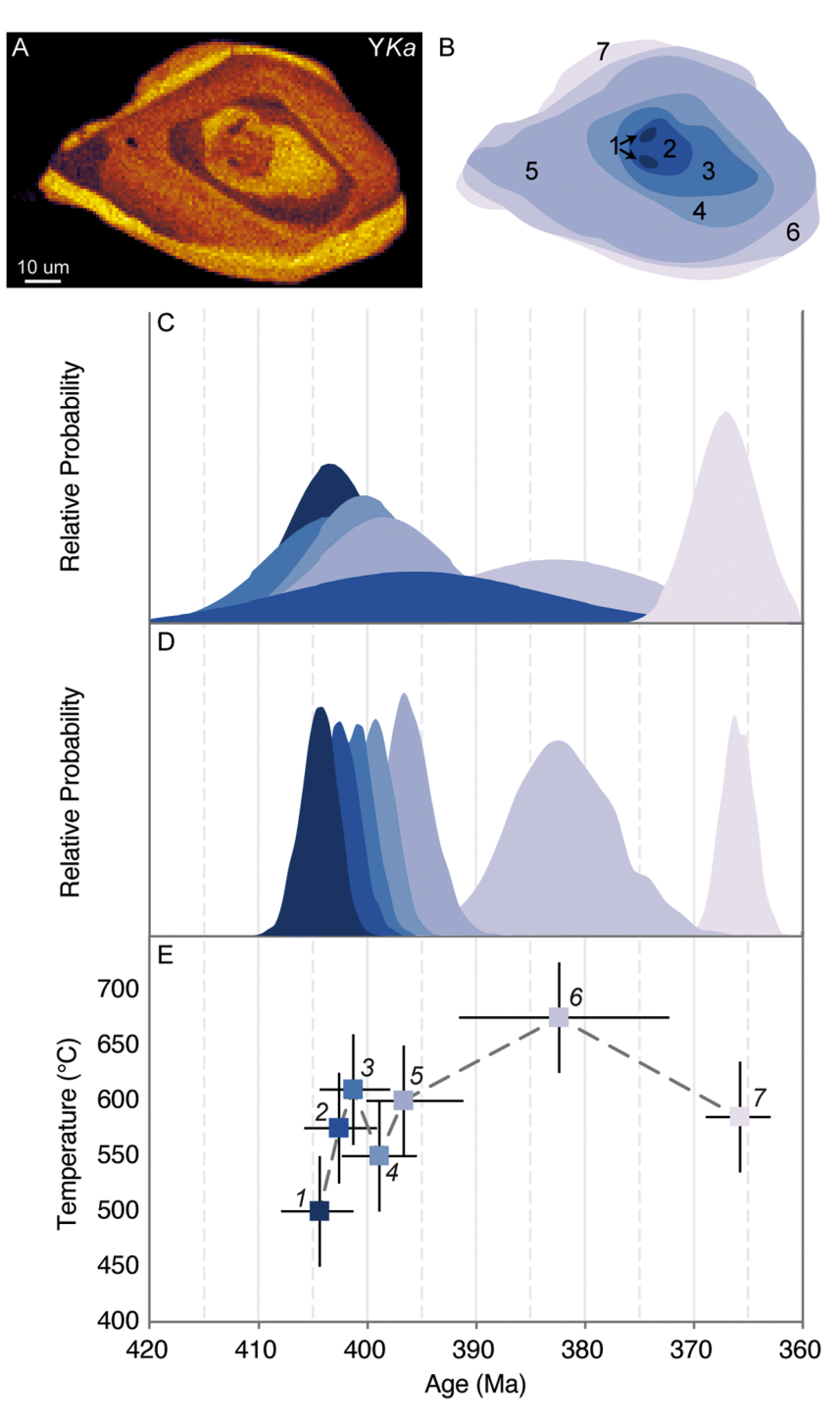


Fig. 1. Application of Bayesian age-sequence modeling to monazite petrochronologic data from sample 21IWH01 of Hillenbrand et al. (2023a) from the Amherst block, New England Appalachians. (A) Yttrium compositional X-ray map of representative monazite grain from Hillenbrand et al. (2023a). (B) Sketch of monazite grain highlighting compositional domains one through seven. (C) Geochronologic results displaying the weighted mean U-Th-Pb_{total} date of each compositional domain as a Gaussian distribution. (D) Probability density plot of monazite dates refined by Bayesian age-sequence analysis. (E) Time-temperature plot integrating monazite dates constrained by Bayesian analysis with monazite-xenotime thermometry reported in Hillenbrand et al. (2023a).

processes. These case studies highlight the benefits and added insight provided by Bayesian analysis to temperature-time paths, the timescales of partial melting, and duration of garnet stability.

3.1. Constraining thermal histories

Pressure-temperature-time (P-T-t) paths are key data used to constrain tectonic histories, intensity of metamorphic events, and juxtaposition of terranes (Foster et al., 2004; Harrison et al., 1989; Pyle et al., 2005; Spear, 1993). The exchange of rare earth elements, particularly Y, between monazite and xenotime is highly temperature dependent and has been empirically calibrated as a thermometer (Heinrich et al., 1997; Pyle et al., 2001), as has the exchange of Y between garnet and monazite (Heinrich et al., 1997; Pyle et al., 2001) and xenotime (Pyle and Spear, 2000). As the thermally-activated diffusion rates of Y in monazite, xenotime, and garnet are extremely sluggish (Carlson, 2012; Engi, 2017; Williams et al., 2007), compositional domains are interpreted to record the temperature at the time of formation. This permits the recovery of T-t histories in polymetamorphic or high-grade terranes not resolved by conventional thermobarometric or thermochronologic methods.

3.1.1. Compositionally zoned monazite

Sample IWH20–1 is a schist from the northern Appalachian Mountains with a peak assemblage that includes biotite, muscovite, garnet (Alm_{72–66}Pyr_{13–4}Sps_{12–28}Grs₃), quartz, plagioclase (An_{19–24}), and sillimanite (Hillenbrand et al., 2023a). The sample was collected from the Amherst block, an inlier of Paleozoic metamorphic rocks within the Mesozoic Hartford basin, which has been interpreted as a high-level thrust nappe that experienced Paleozoic metamorphism and then was down-dropped during Mesozoic extension (Robinson et al., 1998). Peak metamorphic conditions have been estimated at 0.45 \pm 0.1 GPa, 650 \pm 50 °C (Hillenbrand et al., 2023a).

Monazite crystals in sample IWH20–1 are complexly but systematically zoned with up to seven concentric domains defined by Y, labeled domains 1–7 from core to rim (Fig. 1A-B). Domains one through seven yielded weighted mean dates of 403 \pm 4, 395 \pm 12, 403 \pm 6, 400 \pm 5, 398 \pm 6, 382 \pm 10, and 366 \pm 3 Ma (Fig. 1C; Table 1) (Hillenbrand et al., 2023a). The consistent, systematic, concentric monazite zoning supports the application of Bayesian age-sequence modeling using the order of domains as a prior and assuming core to rim growth. This approach yielded dates of 404 $^{+4}/_{-3}$, 403 $^{+3}/_{-4}$, 401 \pm 3, 399 \pm 3, 397 $^{+3}/_{-6}$, 382 $^{+9}/_{-10}$, and 366 \pm 3 Ma (Fig. 1D; Table 1). Notably, the Bayesian model resulted in the reduction of uncertainties for several of the domains by 3 to 9 myr (40–70 %) with some asymmetric uncertainties. Based upon microstructural analysis and overlapping dates, Hillenbrand et al. (2023a) concluded that each monazite domain was in equilibrium with xenotime, enabling the use of monazite-xenotime thermometry.

Fig. 1E shows calculated monazite-xenotime temperatures paired with the dates refined by Bayesian modeling. The data (tabulated in Table 1) indicate heating from \sim 500 to \sim 610 °C between 404 $^{+4}/_{-3}$ and

Table 1Summary of age-sequence modeling and monazite-xenotime thermometry of monazite from sample IWH20–1.

Monazite domain	Weighted mean date (Ma $\pm 2\sigma$)*	Bayesian model date (Ma $\pm 2\sigma$)	Mnz-Xtm T ($^{\circ}$ C \pm 50)	Rate (°C/myr)
1	403 ± 4	404 +4/_3	500	_
2	395 ± 12	$403^{+3}/_{-4}$	575	+42
3	403 ± 6	401 ± 3	610	+26
4	400 ± 5	399 ± 3	550	-25
5	398 ± 6	$397^{+3}/_{-6}$	600	23
6	382 ± 10	$382^{+9}/_{-10}$	675	+5
7	366 ± 3	366 ± 3	585	-5

^{*} Weighted mean dates presented in Hillenbrand et al. (2023a).

 401 ± 3 Ma, followed by cooling to $\sim\!550$ °C by 399 ± 3 Ma. Then, the rocks reached a peak temperature of $\sim\!675$ °C at $382^{+9}/_{-10}$ Ma followed by cooling through $\sim\!590$ °C by 366 ± 3 Ma. The ca. 403 and 380 Ma thermal peaks recorded by this sample correspond regionally with peak metamorphism associated with the Acadian and Neoacadian orogenies, respectively (Robinson et al., 1998). Overall, the (P-)T-t path is similar to that inferred from the Chesham Pond nappe in New Hampshire (Pyle et al., 2005). Notably, the second period of cooling involved much slower rates ($\sim\!5$ °C/myr) than the first phase ($\sim\!15$ °C/myr). Slow cooling ($\sim\!2-5$ °C/myr) associated with the Neoacadian orogeny is also indicated by $^{40}{\rm Ar}/^{39}{\rm Ar}$ thermochronology (Harrison et al., 1989; Hillenbrand et al., 2021) and geospeedometry (Tracy and Dietsch, 1982).

3.1.2. Inclusions within zoned minerals

Age-sequence modeling can also be applied to zoned nonchronometer minerals or inclusions within minerals which show a relative age progression. Sample P101A of Hillenbrand et al. (2023a, 2021) from the central Massachusetts metamorphic high is a paragneiss with the peak assemblage biotite, garnet (Alm₆₈₋₇₀Pyr₂₆₋₂₄Sps₃Grs₃₋₂), quartz, plagioclase (An₂₅₋₁₁), sillimanite, and K-feldspar with accessory rutile, apatite, zircon, monazite, and xenotime. Garnet crystals are zoned in terms of both composition and inclusion characteristics. Garnet cores have relatively high CaO (\sim 1.05 wt%) and Y (0.04–0.09 wt%) and are separated from a lower CaO (\sim 0.85–0.95 wt%) and Y (<0.03 wt%) rim by a relatively high CaO (~1.15 wt%) annulus (Fig. 2A) (Hillenbrand et al., 2023a). Xenotime is found as inclusions in the garnet core, inwards of the high-Y annulus, while monazite is included in the garnet rim, outward of the annulus (Fig. 2A). These inclusions are interpreted as primary because they are included fully within the garnet and do not intersect fractures. The core to rim constraint of garnet growth (Baxter et al., 2017) requires that inclusions in the core predate those in the rim (Foster et al., 2004).

The weighted mean dates of xenotime inclusions in garnet cores (382 \pm 10 Ma) and monazite inclusions with garnet rims (384 \pm 6 Ma) overlap within uncertainty (Table 2) (Hillenbrand et al., 2023a, 2021). Applying the geometric constraint of garnet growth as a prior constraint in Bayesian analysis yielded dates of 386 $^{+8}/_{-6}$ Ma for xenotime in the garnet core and 383 $^{+5}/_{-6}$ Ma for the monazite included in the garnet rim. Hillenbrand et al. (2023a), carried out quantitative thermometry by pairing monazite and xenotime with the composition of the associated garnet domains. Xenotime-garnet thermometry of the garnet core yielded a $\sim\!530\,^{\circ}\text{C}$ estimate and monazite-garnet thermometry of the garnet rim yielded 650–725 $^{\circ}\text{C}$ temperatures (Table 2). Combining thermometry with the dates refined by Bayesian modeling yields an apparent heating rate of 240 $^{+5}/_{-230}\,^{\circ}\text{C}$.

3.1.3. Reaction dating

Dating specific generations of chronometer phases associated with metamorphic reactions provides direct timing constraints on segments of the pressure-temperature path. Hence, "reaction dating" is increasingly becoming the focus of many researchers to characterize the timing and duration of metamorphic, igneous, and fluid-related events (Baxter et al., 2017; Hillenbrand et al., 2023a, 2023b; Pyle et al., 2005; Williams et al., 2019, 2017; Yakymchuk et al., 2017).

3.1.4. Constraining the timescales of partial melting

The timing and duration of partial melting are important because of the implications for rheology, strain localization, petrogenesis of associated igneous rocks, differentiation of the continental crust, and tectonic histories in general (Beaumont et al., 2006; Spear, 1993; Spear et al., 1999; Yakymchuk et al., 2017). Monazite is commonly used as a monitor of the timing of partial melting because, in rocks where monazite and garnet are the only Y-bearing phases, changes in Y concentrations in monazite can be linked to (peritectic) garnet growth (Mahan et al., 2006; Pyle et al., 2005; Williams et al., 2017).

Sample 21IWH16 is a migmatitic paragneiss sampled from drill core

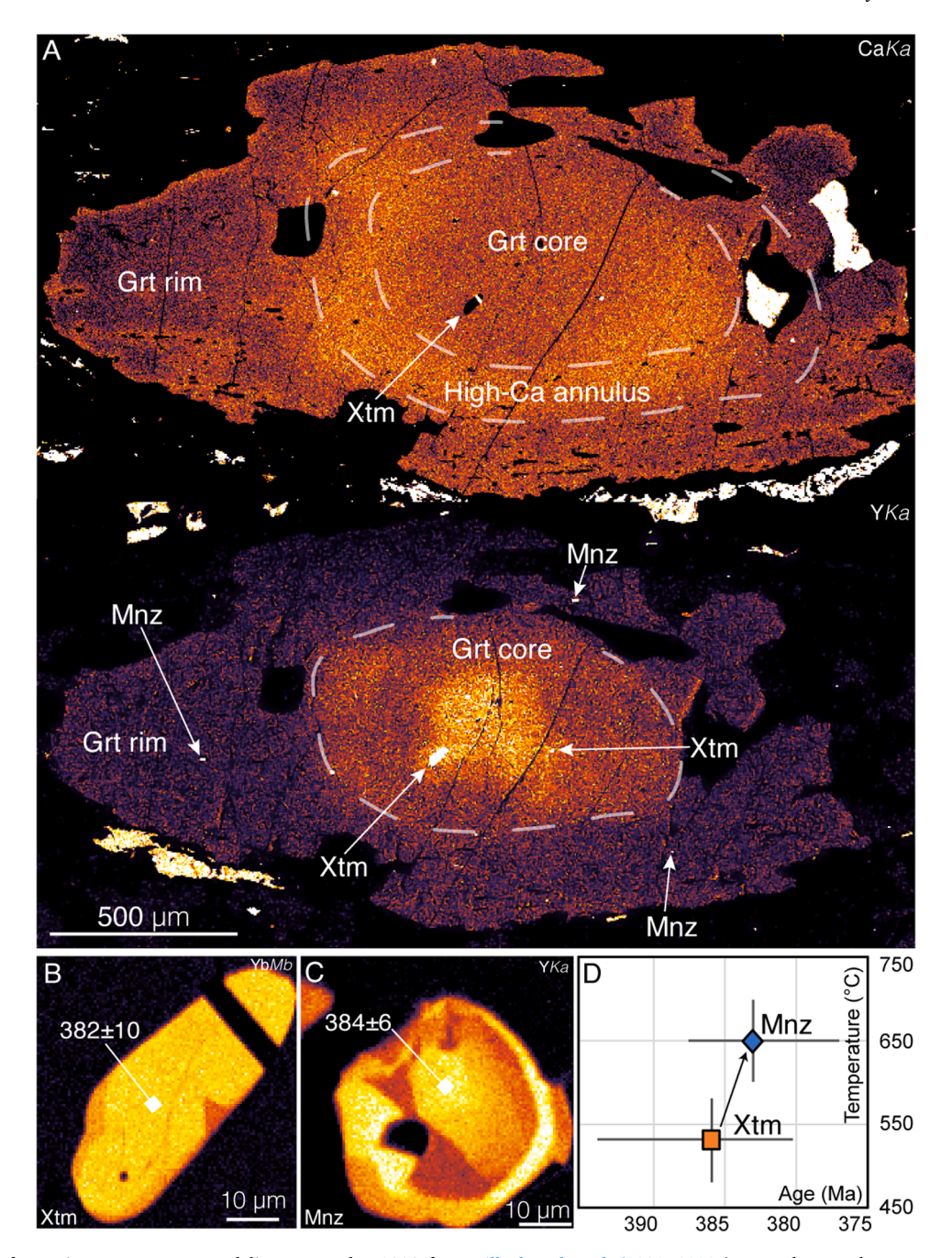


Fig. 2. Application of Bayesian age-sequence modeling to sample P101A from Hillenbrand et al. (2021; 2023a), central Massachusetts metamorphic high, New England Appalachians. (A) Calcium and Yttrium X-ray compositional maps of garnet from sample P101A highlighting xenotime and monazite inclusions in the core and rim, respectively. (B) Ytterbium X-ray compositional map of xenotime included in garnet labeled with U-Th-Pb_{total} date. (C) Yttrium X-ray compositional map of monazite included in garnet labeled with U-Th-Pb_{total} date. (D) Time-temperature plot integrating monazite dates constrained by Bayesian analysis with the results of xenotime-garnet and monazite-garnet thermometry reported in Hillenbrand et al. (2023a). Abbreviations: Grt: garnet, Mnz: monazite, Xtm: xenotime.

Table 2Age sequence modeling of garnet inclusions from sample P101A.

Domain Analyzed	Weighted mean date (Ma $\pm 2\sigma$)	Bayesian model date (Ma $\pm 2\sigma$)	Thermometry ($^{\circ}\text{C} \pm 50$)	Rate (°C/ myr)
Xenotime in garnet core	382 ± 10	$386^{+8}/_{-6}$	530	-
Monazite in garnet rim	384 ± 6	$383\ ^{+4}/_{-6}$	650–725	$240^{+5}/_{-230}$

in the southern Trans-Hudson orogen (Hillenbrand et al., 2024a, 2024b). The sample experienced peak conditions of >900 °C, >1.0 GPa based upon phase equilibria modeling and ternary feldspar thermometry (Hillenbrand et al., 2024a). It has an assemblage that includes K-feldspar (Or_{94–97}; ~39.0 %), quartz (~28.9 %), biotite (~21.9 %), perthite (exsolved ternary feldspar; An_{5–10}Ab_{19–37}Or_{54–76}; ~8.0 %), garnet (Alm_{81–82}Grs₂Py_{14–13}Sps₄; ~2.1 %), and plagioclase (Ab_{94–98}; ~0.1 %) with accessory rutile, apatite, monazite, zircon, and xenotime. The peak metamorphic assemblage is inferred to be ternary feldspar, quartz, rutile, and melt with or without biotite. This assemblage and the rarity or absence of plagioclase, sillimanite, and peak biotite indicate that a reaction such as biotite + plagioclase + aluminosilicate + quartz =

garnet + K-feldspar + melt was exceeded (Mahan et al., 2006; Spear et al., 1999; Williams et al., 2019).

Monazite occurs as both inclusions in garnet and as a matrix phase. Here we focus on the complexly zoned matrix grains; description and interpretation of monazite included in garnet is provided in Hillenbrand et al. (2024a). Up to five compositional domains are observed in matrix monazite crystals (Fig. 3A), referred to as domains one through five from core to rim. From monazite domain one to two, the concentration of Y decreases from ~22,000 to 2100 ppm and the Eu anomaly (Eu/Eu*) decreases from 0.25 to 0.13 and Sr increases from 30 to 110 ppm. Monazite domain three is characterized by relatively low Y (~2400 $\,$ ppm) and oscillatory Th-zoning. Yttrium increases to \sim 9000 ppm and ~22,000 ppm in domains four and five, respectively. Weighted mean U-Th-Pbtotal dates calculated for matrix monazite are visualized as Gaussian distributions in Fig. 3B and summarized in Table 3. The weighted mean dates of each are, domain one: 1868 \pm 10 (n = 3; MSWD=0.1); domain two: 1873 ± 5 (n = 3; MSWD=0.2); domain three: 1842 \pm 9 (n = 4, MSWD=2); domain four: 1852 \pm 4 (n = 4; MSWD=0.7); domain five: 1814 ± 6 Ma (n = 4; MSWD=0.7). Bayesian age sequence modeling of these domains yielded dates of $1873^{+8}/_{-5}$, $1872^{+4}/_{-5}$, $1852^{+5}/_{-4}$, 1850 ± 4 , and $1813^{+5}/_{-7}$ Ma for domains one through five (Table 2; Fig. 3C). Domains one through three can be closely linked with the history of partial melting based upon microstructures and composition. The reader is referred to Hillenbrand et al. (2024a) for a more detailed description and interpretation of the other domains.

Low-Y domain-one monazite $(1873^{+8}/_{-5} \text{ Ma})$ occurs as cores in matrix monazite and as well as inclusions within garnet. The high-Y concentrations of this population (Fig. 3A, D) suggest crystallization prior to significant garnet growth (Foster et al., 2000; Williams et al., 2017). Monazite-xenotime thermometry of domain-one monazite, paired with co-existing xenotime grains, yielded 625–650 \pm 50 $^{\circ}$ C temperatures. The depletion of Y and Eu/Eu* and enrichment in Sr in monazite domain-two (Fig. 3D) is consistent with its crystallization during or after biotite-dehydration melting (>750 °C), as this reaction produces peritectic garnet and K-feldspar, which sequester Y and Eu, respectively, and consumes plagioclase, the breakdown of which releases Sr (Mahan et al., 2006; Williams et al., 2019, 2017). Bayesian modeling indicates a difference of $0.5^{+9}/_{-0.4}$ myr between monazite domains one and two, suggesting relatively rapid heating rates associated with biotite-dehydration melting (Table 3). The oscillatory zoning displayed by monazite domain three is consistent with crystallization from anatectic melts (Dumond et al., 2008; Kohn et al., 2005; Williams et al., 2019). This interpretation is supported by an 1850±9 Ma weighted mean $^{207}\text{Pb}/^{206}\text{Pb}$ SHRIMP-RG date (n=41; MSWD=0.4) from anatectic zircon from the same sample (Hillenbrand et al., 2024a). Hence, the interval of $20^{+5}/_{-8}$ myr calculated between monazite domains two and three, i.e. between melting and melt-crystallization, is inferred to constrain the duration of suprasolidus conditions (Table 3). The timescales of heating and suprasolidus conditions provide important constraints on the tectonic setting of ultra-high temperature metamorphism (Jiao et al., 2023). In this case the rapid heating rate and short duration of peak conditions $(20^{+5}/_{-8} \text{ myr})$ are consistent with a back-arc tectonic setting (Jiao et al., 2023; Hillenbrand et al., 2024a).

3.1.5. Duration of garnet stability

The linkage between the concentrations of Y in monazite and garnet has been used extensively in petrochronologic studies to infer the timing of garnet growth and breakdown (Engi, 2017; Foster et al., 2004, 2000; Larson et al., 2022; Williams et al., 2017). Garnet is an almost ubiquitous metamorphic mineral in mid- and deep-crustal metasediments, and widespread garnet growth commonly reflects regional crustal thickening and heating (Baxter et al., 2017; Hillenbrand et al., 2023a; Spear, 1993). The common interpretation is that garnet largely controls the Y (and HREE) budget in the rock and thus, when garnet is growing or stable monazite tends to be depleted in these elements (Williams et al.,

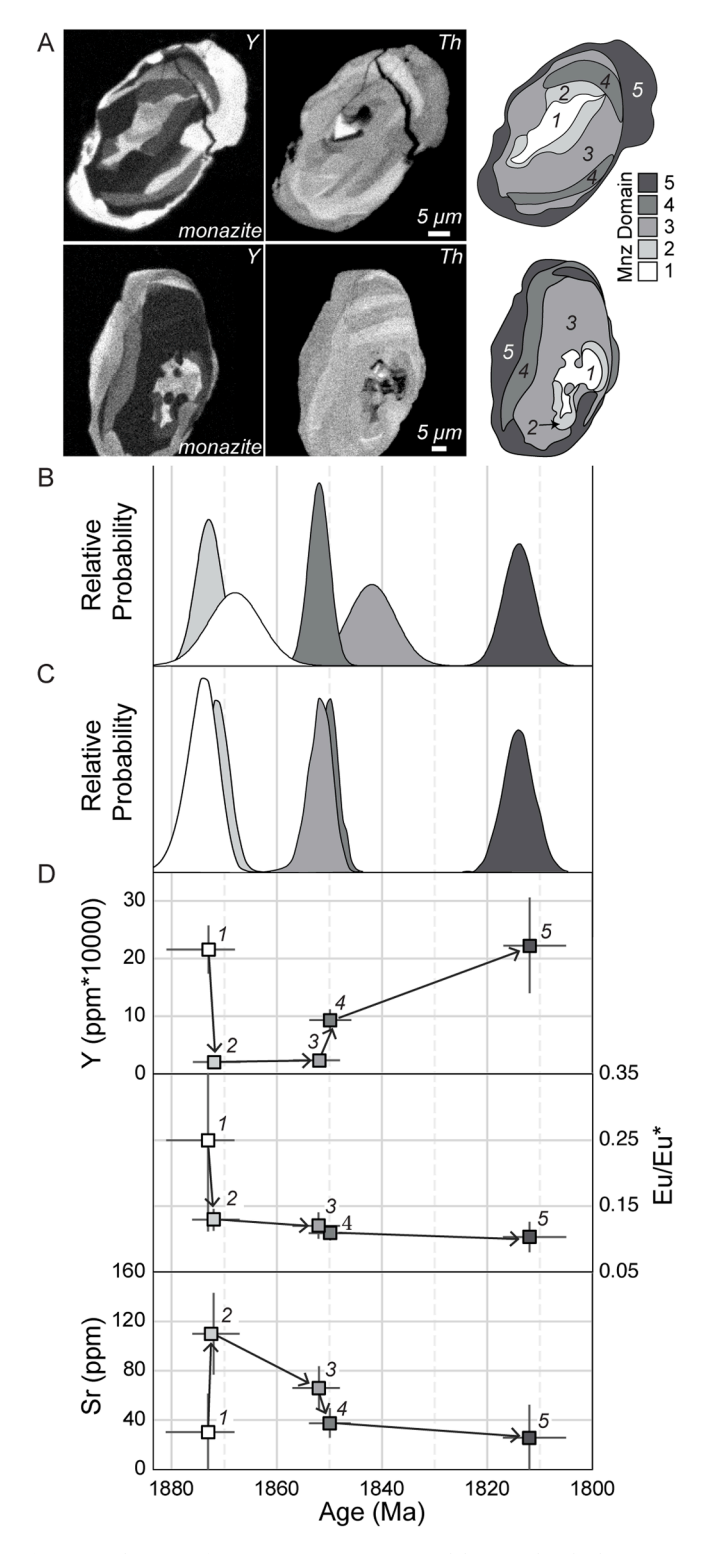


Fig. 3. Application of Bayesian age-sequence modeling to ultra-high temperature paragneiss sample 21IWH16 from the southern Trans-Hudson orogen modified from Hillenbrand et al. (2024a). (A) Yttrium and Thorium X-ray compositional maps and associated sketches of the compositional zoning patterns and domains in matrix monazite. (B) Geochronologic results displaying the weighted mean U-Th-Pb_{total} date of each compositional domain as a Gaussian distribution. (C) Probability density plot of monazite dates refined by Bayesian age-sequence analysis. (D) Bivariate plots showing dates of monazite domains, refined by Bayesian age-sequence modeling, against Y, Eu/Eu*, and Sr compositional data.

Table 3 Summary of age-sequence modeling from sample 21IWH16.

Monazite domain	Weighted mean date (Ma $\pm 2\sigma$)	Bayesian posterior date (Ma $\pm 2\sigma$)	Duration (Ma)
1	1868±10	$1873^{+8}/_{-5}$	_
2	1873 ± 5	$1872^{+4}/_{-5}$	$0.5^{+9}/_{-0.4}$
3	1842 ± 9	$1852^{+5}/_{-4}$	$20^{+5}/_{-8}$
4	1852 ± 4	1850±4	$0.4^{+6}/_{-0.3}$
5	1814 ± 6	$1813^{+5}/_{-7}$	$35^{+8}/_{-6}$

2017). Similarly, widespread garnet-consuming reactions can indicate decompression, cooling, and fluid influx. As garnet breaks down, it releases Y (and HREE), which leads to elevated monazite Y concentrations. Hence, the duration of low-Y monazite has been widely used as a proxy for the stability of garnet (Foster et al., 2000; Mahan et al., 2006; Spear and Pyle, 2010; Williams et al., 2017). Many studies have interpreted inflection points in petrochronologic data (i.e., monazite-Y patterns) by visual inspection (e.g. Markley et al., 2018; Williams et al., 2019; Hillenbrand et al., 2021), although this approach is less quantitative and lacks robust uncertainty estimates.

The changes commonly observed in monazite composition can be quantified using change point analysis, a statistical method used to identify and analyze changes or shifts in a dataset over time. This analysis can be applied using a Bayesian framework, using prior information, such as the domains observed in compositional maps to inform the number of change points. Then, a Markov Chain-Monte Carlo (MCMC) approach is used to estimate uncertainties. The combination of Bayesian change point analysis with MCMC allows the incorporation of prior information to place quantitative constraints on complex petrochronologic datasets with robust uncertainty estimation.

We illustrate the utility of this method with an example from New England, USA. The southern New England Appalachians are well known for having contrasting P-T paths associated with the Devonian to Carboniferous (Neo)Acadian orogeny (Armstrong et al., 1992; Spear, 1993). West of the Mesozoic Hartford basin, P-T paths are clockwise while east of the Hartford basin counterclockwise paths are characteristic, particularly in the central Massachusetts metamorphic high (Fig. 4A) (Armstrong et al., 1992; Hillenbrand et al., 2023a; Thomson, 2001). These contrasting paths may reflect differences in the structural position in the orogen, as rocks west of the Hartford basin formed the orogenic retrowedge whereas the central Massachusetts metamorphic high may represent the orogenic core (Hillenbrand et al., 2023a). Despite contrasting P-T paths, monazite from garnet-bearing metapelitic rocks from both domains have similar zoning: high-Y cores, low-Y mantles, and high-Y rims. The monazite domains have been interpreted to reflect monazite growth (1) prior to significant garnet crystallization, (2) in the presence of stable garnet, and (3) during garnet breakdown, respectively (Hillenbrand et al., 2021, 2023a).

The Straits Schist is a Silurian-Devonian metapelitic rock unit located west of the Hartford basin. Previous ca. 410-355 Ma ID-TIMS and LA-ICP-MS U-Pb monazite, zircon, and garnet dates have been interpreted to record metamorphism associated with the (Neo)Acadian orogeny (Lanzirotti and Hanson, 1996, 1995; Millonig et al., 2020). These dates, while yielding constraints on the timing and timescales of regional metamorphism, lack paired compositional data, making it difficult to link monazite age information to P-T conditions as well as to garnet growth and breakdown. Hillenbrand et al. (2023b) reported U-Th-Pbtotal monazite dates and compositions from two garnet-bearing samples of The Straits Schist. These samples have peak assemblages with muscovite, biotite, quartz, garnet (Alm₅₃₋₇₆Pyr₃₃₋₁₅Sps₂₂₋₂Grs₂₁₋₇), kyanite, and plagioclase (An₁₆₋₂₂) with accessory ilmenite, apatite, zircon, monazite, and xenotime (Hillenbrand et al., 2023b). Petrogenetic grid analysis, internally consistent multi-equilibria thermobarometry, and Gibbs modeling indicate a clockwise P-T path involving burial and heating from 550 °C at 0.5 GPa to 700 °C at 1.0 GPa, followed by

retrogression to 0.4–0.6 GPa at 540–590 °C (Fig. 4a) (Armstrong et al., 1992; Hillenbrand et al., 2023b). The samples yielded consistent monazite zoning patterns characterized by three compositional domains: moderate-Y cores (4000–8000 ppm), low-Y mantles (500–1900 ppm), and high-Y rims (15,000–22,000 ppm). Cores yielded a weighted mean date of 393±4 Ma, mantles yielded dates of 380±4 Ma and 386±4 Ma, and rims have been dated at 378±5 and 377±4 Ma (Hillenbrand et al., 2023b). Bayesian modeling yielded the first change point, with decreasing Y from higher-Y cores to low-Y mantles, at $384^{+8}/_{-9}$ Ma. The second change point, associated with increasing Y from mantles to rims, is constrained to $375^{+4}/_{-12}$ Ma. Rhat values of 1.0–1.1 for both change points (Table 4) indicates that the MCMC chains have converged.

The central Massachusetts metamorphic high is a broad region of upper amphibolite to granulite facies metamorphic rocks exposed from northern Connecticut to southern New Hampshire east of the Hartford basin (Robinson et al., 1998; Thomson, 2001). A relatively large monazite petrochronology dataset has been developed from the central Massachusetts metamorphic high (Hillenbrand et al., 2021; Massey et al., 2017). Visual inspection has been used to suggest a decrease in Y from \sim 20,000 to <500 ppm at ca. 380–370 Ma and an increase in Y to ~800-20,000 ppm at ca. 340-330 Ma (Hillenbrand et al., 2021). Bayesian change point analysis with MCMC of this dataset yielded an initial change point at $375^{+2}/_{-4}$ Ma associated with a decrease in Y from monazite cores to mantles (Rhat=1.0). A second change point, 345⁺¹³/₋₁₅ Ma, is associated with increasing Y, linked with garnet breakdown (Rhat=1.1). These results are consistent with visual inspection of composition vs date plots (e.g. Hillenbrand et al., 2021) and add more robust uncertainty estimates on monazite compositional

Bayesian analysis highlights the dramatic differences in the duration of low-Y monazite and garnet stability east and west of the Hartford basin: approximately 9 myr west of the Hartford basin and approximately 30 myr to the east. As the duration of low-Y monazite is commonly linked to the duration of garnet stability and thus residence at depth, it suggests that the rocks east of the Hartford basin in the central Massachusetts metamorphic high experienced a more prolonged tenure at (near-) peak pressures. This is compatible with the counterclockwise P-T path and very slow cooling rates (2-5 °C/myr) indicated by existing petrologic, thermochronologic, and geospeedometric studies in this region (Armstrong et al., 1992; Dietsch et al., 2010; Hames et al., 1989; Hillenbrand et al., 2023a; Tracy and Dietsch, 1982). The change points also indicate differences in the absolute timing of garnet growth and breakdown. The calculations suggest earlier garnet growth and breakdown in rocks west of the Hartford basin relative to those to the east (Table 4).

4. Implications

4.1. Formally integrating geologic and petrologic observations with geochronology

Relative age constraints provided by cross cutting relationships, compositional zoning, and petrologic phase relationships have long been used to infer the relative order of geologic processes, metamorphic reactions, and the growth of mineral domains. Bayesian statistics provides a means to formally incorporate relative constraints into petrochronologic analysis. Formalized Bayesian "age-sequence" modeling allows for the direct estimation of the ages and uncertainties of minerals or mineral domains while incorporating constraints from geologic and petrologic observations. This approach is, in many ways, analogous to those applied in lower temperature geologic systems. Bayesian modeling of sedimentary successions incorporates the law of stratigraphic superposition and information from multiple age constraints (e.g. detrital zircon maximum depositional ages, direct dates of ash beds, astrochronology, and biostratigraphic data) to yield refined posterior chronologies (Johnstone et al., 2019; Trayler et al., 2019, 2024). Similarly,

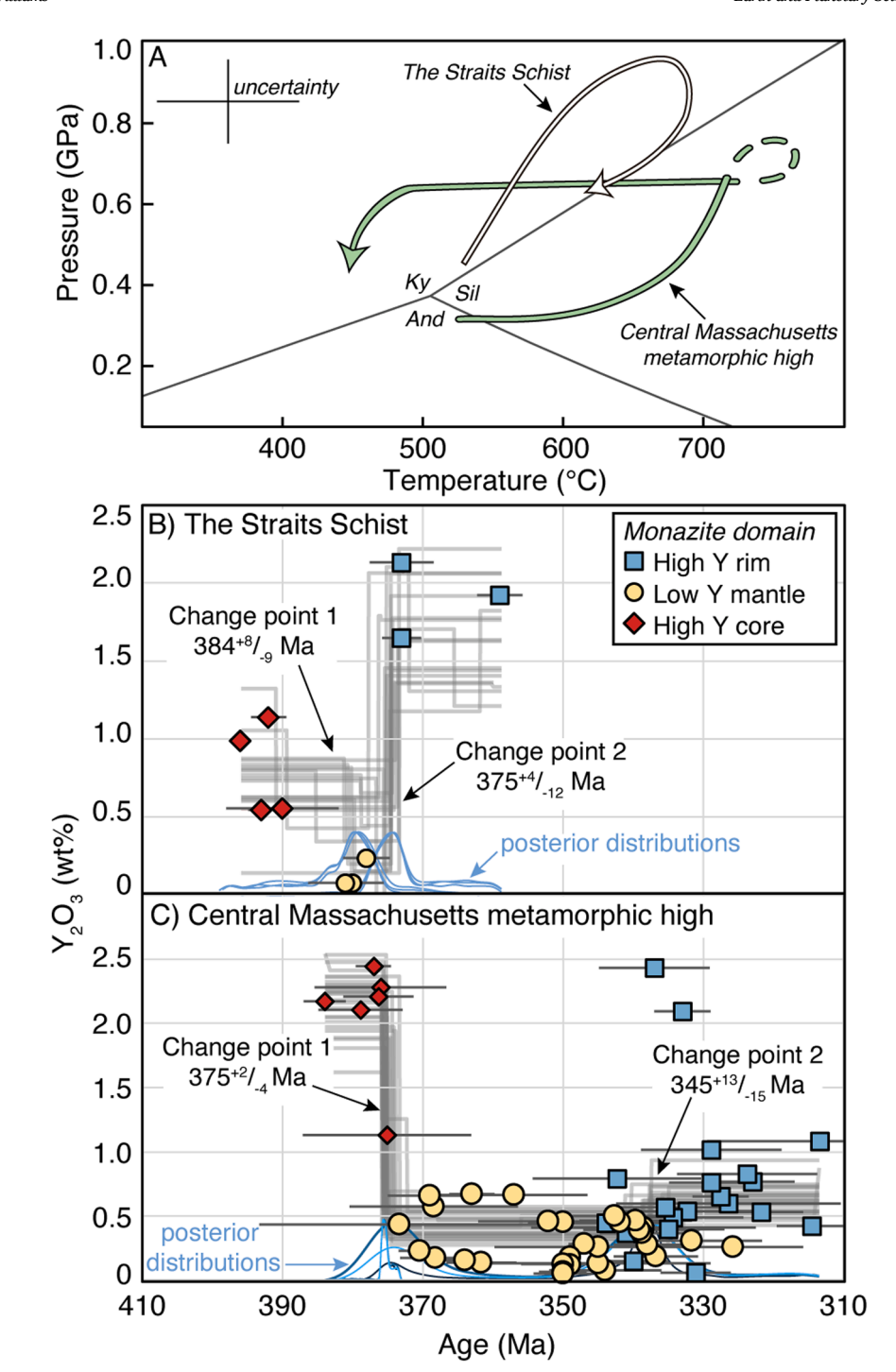


Fig. 4. Application of Bayesian Markov chain-Monte Carlo (MCMC) change point analysis to petrochronologic data from the New England Appalachians. (A) Representative P-T paths for the central Massachusetts metamorphic high (Thomson, 2001; Hillenbrand et al., 2023a) and The Straits Schist (Hillenbrand et al., 2023b). (B) Bayesian change point analysis of monazite data from The Straits Schist annotated with change points. (C) Bayesian change point analysis of monazite data (Hillenbrand et al., 2021) from the central Massachusetts metamorphic high highlighting change points. Gray lines through the data point represent fitted lines drawn randomly from the posterior. Blue lines are the change point posterior density distributions for each MCMC chain (For interpretation of the references to color in this figure legend, the reader is referred to the web version of this article).

Table 4 Summary of change point analysis.

The Straits Schist			Central Massachusetts m	Central Massachusetts metamorphic high		
Compositional change point	Change point (Ma)	Duration (Ma)	Rhat*	Change point (Ma)	Duration (Ma)	Rhat*
1: Decrease in Y	$384^{+8}/_{-9}$	_	1.1	$375^{+2}/_{-4}$	_	1.0
2: Increase in Y	$375^{+4}/_{-12}$	$9^{+12}/_{-13}$	1.0	$345^{+13}/_{-15}$	$30^{+15}/_{-19}$	1.1

^{*} Gelman and Rubin's convergence diagnostic.

thermal history models for low temperature thermochronology incorporate prior geologic constraints for more precise and accurate models (Flowers et al., 2015). Our approach incorporating prior petrologic information in high-temperature systems can lead to more refined chronologies at spatial scales ranging from individual minerals to broad regions.

One important aspect of Bayesian age-sequence modeling is the reduction of uncertainties on geochronologic dates. Relative precision is increased most where a clear relative age progression is observed across multiple compositional domains with overlapping dates. Lesser amounts of relative precision are gained in cases where dates are already resolved within uncertainty, although the Bayesian analysis may provide more robust estimates of the uncertainties and the intervals between domains. This approach is illustrated by Farrell et al. (2024) who estimate garnet growth rates using Bayesian model incorporating the geometric constraint of core to rim growth. Thus, Bayesian age-sequence modeling can provide temporal resolution where domains cannot be resolved within analytical uncertainty.

4.2. Monazite compositional profiles: constraints on tectonic histories

Bayesian change point analysis provides a statistical framework in which to constrain the timing and significance of compositional domains in chronometer phases (monazite, xenotime, zircon, titanite, garnet, etc.). The compositional changes likely signal changes in metamorphic reactions and/or assemblages providing a direct linkage between chronology and petrologic history (Foster et al., 2004, 2000; Kohn et al., 2005; Williams et al., 2019; Larson et al., 2022; Farrell et al., 2024). As shown in Fig. 5A, modified from Hillenbrand et al. (2023b), domains with different tectono-metamorphic histories have different durations of low-Y monazite. Because garnet and monazite are typically the main Y hosts in xenotime-absent metapelites (Spear and Pyle, 2010), profiles of Y vs. date have a characteristic shape that can represent the period of garnet stability (crustal thickening?) in orogenic rocks (Williams et al., 2019; Hillenbrand et al., 2021, 2023a).

Durations of garnet stability in amphibolite to granulite facies rocks may range from <10 to several 10 s of myr or more. This variation has been noted in many orogenic belts including the Grenville Province (Markley et al., 2018; Williams et al., 2019; Regan et al., 2019), southwest U.S.A. (Daniel and Pyle, 2006), Trans-Hudson orogen (Copley and Weller, 2022; Dahl et al., 2005), and Athabasca granulite terrane, Saskatchewan (Dumond, 2020; Dumond et al., 2008; Mahan et al., 2006). Broadly, two types of Y concentration vs monazite date profile can be recognized: one in which garnet breakdown swiftly follows garnet growth and another in which garnet is stable for a prolonged

period. We refer to these as "V" and "U" shaped profiles, respectively, referring to the age vs Y in monazite time sequence (Fig. 5). V-shaped profiles are predicted by classic numerical models of Barrovian-style metamorphism and predict burial, peak conditions, and exhumation over timescales on the order of 5-15 myr (Fig. 5B) (Copley and Weller, 2022; England and Thompson, 1984a, 1984b). In contrast, U-shaped profiles involve more protracted metamorphism and durations of garnet stability that require long-term residence at garnet-stable pressures, i.e. the middle or lower crust (Fig. 5C) (Hillenbrand et al., 2023a; Mahan et al., 2006; Williams et al., 2019). We propose that U-shaped profiles are characterized by durations of garnet stability on the order of 20 myr or more as these timescales exceed the typical middle to deep crustal residence predicted by many numerical models for Barrovian-style metamorphism (England and Thompson, 1984a, 1984b; Jamieson et al., 1998). This may reflect protracted deep burial within the middle to lower crust of an orogenic belt where sustaining a thickened, rheologically weak crust requires continued compressional stress and a balance of erosion and shortening. Alternatively, rocks may experience deep crustal residence during and after an orogenic event (e.g. Ellis, 1987; Mahan et al., 2006; Dumond, 2020). In both scenarios, the rocks are likely exhumed in a subsequent tectonic event following prolonged deep crustal residence (Ellis, 1987; Harley, 1989). Change point analysis provides quantitative constraints on the duration of garnet stability, which in turn, can be used to compare these processes across samples, regions within an orogen, or across different orogens. This metric can provide a more objective and reproducible set of interpretations than subjective visual inspection alone.

5. Conclusions and future directions

Bayesian statistical analysis provides an exciting avenue to refine the timescales of geologic processes and strengthen tectonic interpretations. While we have focused primarily on applications to accessory mineral petrochronology, this approach could be applied to virtually any dateable mineral phase or rock sequence that shows textural, microstructural, and/or compositional evidence of a relative age progression. Future directions for age-sequence modeling may include the incorporation of additional priors such as constraints on the rates of metamorphic reactions, crystal growth, deformation, or dissolution-reprecipitation processes, geospeedometry, or more detailed textural fabric-related constraints such as the stages of crenulation cleavage development. Moving forward, change point analysis may also incorporate more complex priors and multi-variate regression of several elements to further tie dates with geologic reactions and processes. We emphasize that this approach provides a formalism to integrate the

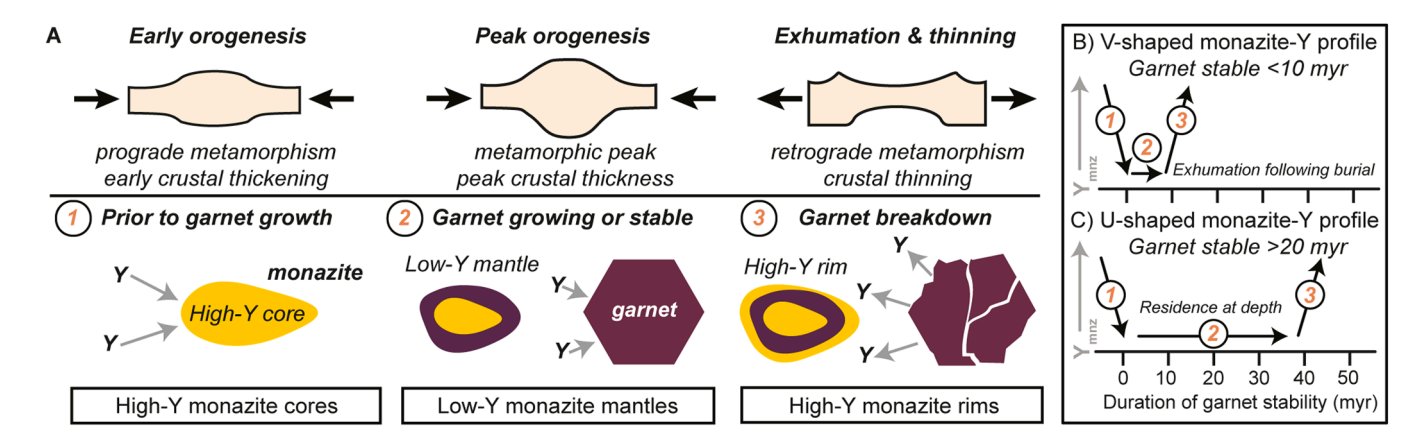


Fig. 5. (A) Relationship between orogenic evolution (top row) and reactions involving monazite and garnet (bottom row) adapted from Hillenbrand et al. (2023a). (B) Schematic sketch of monazite age vs Y composition in a sample with a relatively short (<20 myr) duration of garnet stability referred to here as a "V-shaped" profile. (C) Schematic sketch of monazite age vs Y composition in a sample with a relatively long duration (>20 myr) of garnet stability referred to here as a "U-shaped" profile.

relative age constraints routinely noted as part of geologic and petrologic analysis with geochronologic data and, while not necessarily complex, it can provide a more objective and reproducible set of interpretations compared to weighted means or visual inspection.

CRediT authorship contribution statement

Ian W. Hillenbrand: Writing – original draft, Writing – review & editing, Conceptualization, Data curation, Formal analysis, Investigation, Methodology. Michael L. Williams: Writing – review & editing.

Declaration of competing interest

The authors declare that they have no known competing financial interests or personal relationships that could have appeared to influence the work reported in this paper.

Data availability

This study applied Bayesian statistical analysis to previously published data. The data sources are Hillenbrand et al. (2021, 2023a, 2023b, 2024a, 2024b).

Acknowledgments

IWH and MLW were supported by the NSF EAR-1930014. We appreciate helpful discussions with Amy Gilmer as well as presentations and discussions with Mark Schmitz which led us to explore Bayesian statistics. We appreciate the editorial guidance of Alexander Webb and constructive scientific reviews from Mark Schmitz and Margo Odlum.

References

- Allaz, J.M., Williams, M.L., Jercinovic, M.J., Goemann, K., Donovan, J., 2019. Multipoint background analysis: gaining precision and accuracy in microprobe trace element analysis. Microsc. Microanal. 25, 30–46. https://doi.org/10.1017/ \$1431927618015660
- Armstrong, T.R., Tracy, R.J., Hames, W.E., 1992. Contrasting styles of Taconian, Eastern Acadian and Western Acadian metamorphism, central and western New England. J. Metamorph. Geol. 10, 415–426. https://doi.org/10.1111/j.1525-1314.1992.
- Baxter, E.F., Caddick, M.J., Dragovic, B., 2017. Garnet: a rock-forming mineral petrochronometer. Rev. Mineral. Geochem. 83, 469–533. https://doi.org/10.2138/
- Beaumont, C., Nguyen, M.H., Jamieson, R.A., Ellis, S., 2006. Crustal flow modes in large hot orogens. Geol. Soc. Lond. Spec. Publ. 268, 91–145. https://doi.org/10.1144/ GSL SP 2006 268 01 05
- Carlson, W.D., 2012. Rates and mechanism of Y, REE, and Cr diffusion in garnet. Am. Mineral. 97, 1598–1618. https://doi.org/10.2138/am.2012.4108.
- Copley, A., Weller, O., 2022. The controls on the thermal evolution of continental mountain ranges. J. Metamorph. Geol. 40, 1235–1270. https://doi.org/10.1111/ img.12664
- Dahl, P.S., Hamilton, M.A., Jercinovic, M.J., Terry, M.P., Williams, M.L., Frei, R., 2005. Comparative isotopic and chemical geochronometry of monazite, with implications for U-Th-Pb dating by electron microprobe: an example from metamorphic rocks of the eastern Wyoming Craton (U.S.A.). Am. Mineral. 90, 619–638. https://doi.org/ 10.2138/am.2005.1382
- Daniel, C.G., Pyle, J.M., 2006. Monazite-Xenotime thermochronometry and Al2SiO5 reaction textures in the Picuris range, Northern New Mexico, USA: new evidence for a 1450-1400 Ma orogenic event. J. Petrol. 47, 97–118. https://doi.org/10.1093/petrology/egi069.
- Dietsch, C., Kunk, M.J., Aleinikoff, J., Sutter, J.F., 2010. The tectono-thermal evolution of the Waterbury dome, western Connecticut, based on U-Pb and ⁴⁰Ar/³⁹Ar ages:. https://doi.org/10.1130/2010.1206(08).
- Dumond, G., 2020. Tibetan dichotomy exposed in the Canadian Shield: a lower crustal perspective. Earth Planet. Sci. Lett. 544, 116375 https://doi.org/10.1016/j. epsl.2020.116375.
- Dumond, G., McLean, N., Williams, M.L., Jercinovic, M.J., Bowring, S.A., 2008. High-resolution dating of granite petrogenesis and deformation in a lower crustal shear zone: athabasca granulite terrane, western Canadian Shield. Chem. Geol. 254, 175–196. https://doi.org/10.1016/j.chemgeo.2008.04.014.
- Engi, M., 2017. Petrochronology based on REE-minerals: monazite, allanite, xenotime, apatite. Rev. Mineral. Geochem. 83, 365–418. https://doi.org/10.2138/rmg.2017.83.12.

- Ellis, D.J., 1987. Origin and evolution of granulites in normal and thickened crusts. Geology 15, 167. https://doi.org/10.1130/0091-7613(1987)15<167:OAEOGI>2.0.
- England, P.C., Thompson, A.B., 1984a. Pressure temperature time paths of regional metamorphism I. heat transfer during the evolution of regions of thickened continental crust. J. Petrol. https://doi.org/10.1093/petrology/25.4.894.
- England, P.C., Thompson, A.B., 1984b. Pressure—temperature—time paths of regional metamorphism II. Their inference and interpretation using mineral assemblages in metamorphic rocks. J. Petrol. 25, 929–955.
- Farrell, T.P., Aerden, D., Baxter, E.F., Starr, P.G., Williams, M.L., 2024. Rapid development of spiral garnets during subduction zone metamorphism revealed from high-resolution Sm-Nd garnet geochronology. Geology 52, 261–265. https://doi. org/10.1130/G51882.1
- Flowers, R.M., Farley, K.A., Ketcham, R.A., 2015. A reporting protocol for thermochronologic modeling illustrated with data from the Grand Canyon. Earth Planet. Sci. Lett. 432, 425–435. https://doi.org/10.1016/j.epsl.2015.09.053.
- Foster, G., Kinny, P., Vance, D., Prince, C., Harris, N., 2000. The significance of monazite U-Th-Pb age data in metamorphic assemblages; a combined study of monazite and garnet chronometry. Earth Planet. Sci. Lett. 181, 327–340. https://doi.org/10.1016/S0012-821X(00)00212-0.
- Foster, G., Parrish, R.R., Horstwood, M.S.A., Chenery, S., Pyle, J., Gibson, H.D., 2004. The generation of prograde P–T–t points and paths; a textural, compositional, and chronological study of metamorphic monazite. Earth Planet. Sci. Lett. 228, 125–142. https://doi.org/10.1016/j.epsl.2004.09.024.
- Hacker, B., Kylander-Clark, A., Holder, R., 2019. REE partitioning between monazite and garnet: implications for petrochronology. J. Metamorph. Geol. 37, 227–237. https:// doi.org/10.1111/img.12458.
- Hames, W.E., Tracy, R.J., Bodnar, R.J., 1989. Postmetamorphic unroofing history deduced from petrology, fluid inclusions, thermochronometry, and thermal modeling: an example from southwestern New England. Geology 17, 727–730. https://doi.org/10.1130/0091-7613(1989)017<0727:PUHDFP>2.3.CO;2.
- Harrison, T.M., Spear, F.S., Heizler, M.T., 1989. Geochronologic studies in central New England II: post-Acadian hinged and differential uplift. Geology 17, 185–189. https://doi.org/10.1130/0091-7613(1989)017<0185:GSICNE>2.3.CO;2.
- Harley, S.L., 1989. The origins of granulites: a metamorphic perspective. Geol. Mag. 126, 215–247. https://doi.org/10.1017/S0016756800022330.
- Haslett, J., Parnell, A., 2008. A simple monotone process with application to radiocarbon-dated depth chronologies. J. R. Stat. Soc. Ser. C (Appl. Stat.) 57, 399–418. https://doi.org/10.1111/j.1467-9876.2008.00623.x.
- Heinrich, W., Andrehs, G., Franz, G., 1997. Monazite-xenotime miscibility gap thermometry. I. An empirical calibration. J. Metamorph. Geol. 15, 3–16. https://doi. org/10.1111/j.1525-1314.1997.t01-1-00052.x.
- Hillenbrand, I.W., Gilmer, A.K., Williams, M.L., Souders, A.K., Jercinovic, M.J., Lowers, H.A., Vazquez, J.A., 2024a. Paleoproterozoic reworking of Archean crust and extreme back-arc metamorphism in the enigmatic southern trans-Hudson Orogen. Geophys. Res. Lett. 51, e2023GL107552 https://doi.org/10.1029/ 2023GL107552.
- Hillenbrand, I.W., Gilmer, A.K., Lowers, H.A., Jercinovic, M.J., Vazquez, J.A., 2024b. Data release of whole rock isotope geochemistry,mineral chemistry, and geochronology for a Proterozoic paragneiss sampled from drill core from North Dakota (Version 1) [Dataset]. Sciencebase. https://doi.org/10.5066/P9VZTGFN.
- Hillenbrand, I.W., Williams, M.L., Heizler, M.T., Jercinovic, M.J., Tjapkes, D.J., Williams, M.L., 2023a. Petrochronologic constraints on Paleozoic tectonics in southern New England. In: Whitmeyer, S.J., Kellett, D.A., Tikoff, B. (Eds.), Laurentia: An Evolving Continent. Geological Society of America. https://doi.org/10.1130/2022.1220(25).
- Hillenbrand, I.W., Williams, M.L., Li, C., Gao, H., 2021. Rise and fall of the Acadian altiplano: evidence for a Paleozoic orogenic plateau in New England. Earth Planet. Sci. Lett. 560. https://doi.org/10.1016/j.epsl.2021.116797.
- Hillenbrand, I.W., Williams, M.L., Peterman, E.M., Jercinovic, M.J., Dietsch, C.W., 2023b. Petrochronologic constraints on inverted metamorphism, terrane accretion, thrust stacking, and ductile flow in the Gneiss Dome belt, northern Appalachian orogen. J. Metamorph. Geol. https://doi.org/10.1002/JMG.12741.
- Jamieson, R.A., Beaumont, C., Fullsack, P., Lee, B., 1998. Barrovian regional metamorphism: where's the heat?. In: Geological Society, 138 Special Publications, London, p. 23. https://doi.org/10.1144/GSL.SP.1996.138.01.03. LP –51.
- Jiao, S., Brown, M., Mitchell, R.N., Chowdhury, P., Clark, C., Chen, L., Chen, Y., Korhonen, F., Huang, G., Guo, J., 2023. Mechanisms to generate ultrahightemperature metamorphism. Nat. Rev. Earth Environ. https://doi.org/10.1038/ s43017-023-00403-2.
- Johnstone, S.A., Schwartz, T.M., Holm-Denoma, C.S., 2019. A stratigraphic approach to inferring depositional ages from detrital geochronology data. Front. Earth. Sci. (Lausanne) 7. https://www.frontiersin.org/articles/10.3389/feart.2019.00057.
- Klein, B.Z., Eddy, M.P., 2023. What's in an age? Calculation and interpretation of ages and durations from U-Pb zircon geochronology of igneous rocks. Geol. Soc. Am. Bull. https://doi.org/10.1130/B36686.1.
- Kohn, M.J., Wieland, M.S., Parkinson, C.D., Upreti, B.N., 2005. Five generations of monazite in Langtang gneisses: implications for chronology of the Himalayan metamorphic core. J. Metamorph. Geol. (23), 399–406. https://doi.org/10.1111/ j.1525-1314.2005.00584.x.
- Kylander-Clark, A.R.C., Hacker, B.R., Cottle, J.M., 2013. Laser-ablation split-stream ICP petrochronology. Chem. Geol. 345, 99–112. https://doi.org/10.1016/j. chemgeo.2013.02.019.
- Lanzirotti, A., Hanson, G.N., 1996. Geochronology and geochemistry of multiple generations of monazite from the Wepawaug Schist, Connecticut, USA: implications

- for monazite stability in metamorphic rocks. Contrib. Mineral. Petrol. 125, 332–340.
- Lanzirotti, A., Hanson, G.N., 1995. U-Pb dating of major and accessory minerals formed during metamorphism and deformation of metapelites. Geochim. Cosmochim. Acta 59, 2513–2526. https://doi.org/10.1016/0016-7037(95)00146-8.
- Larson, K.P., Shrestha, S., Cottle, J.M., Guilmette, C., Johnson, T.A., Gibson, H.D., Gervais, F., 2022. Re-evaluating monazite as a record of metamorphic reactions. Geosci. Front. 13, 101340 https://doi.org/10.1016/j.gsf.2021.101340.
- Lindeløv, J.K., 2020. mcp: An R Package For Regression with Multiple Change Points. OSF Preprints. https://doi.org/10.31219/osf.io/fzqxv.
- Ludwig, K.R., 2003. User's manual for Isoplot 3.00, a geochronological toolkit for Microsoft Excel. Berkeley Geochronol. Cent. Special Publ. 4, 25–32.
- Mahan, K.H., Goncalves, P., Williams, M.L., Jercinovic, M.J., 2006. Dating metamorphic reactions and fluid flow: application to exhumation of high-P granulites in a crustalscale shear zone, western Canadian Shield. J. Metamorph. Geol. 24, 193–217. https://doi.org/10.1111/j.1525-1314.2006.00633.x.
- Markley, M.J., Dunn, S.R., Jercinovic, M.J., Peck, W.H., Williams, M.L., 2018. Monazite U-Th-Pb geochronology of the Central Metasedimentary Belt Boundary Zone (CMBbz), Grenville Province, Ontario Canada. Can. J. Earth. Sci. 55, 1063–1078. https://doi.org/10.1139/cjes-2018-0039.
- Massey, M.A., Moecher, D.P., Walker, T.B., O'Brien, T.M., Rohrer, L.P., 2017. The role and extent of dextral transpression and lateral escape on the post-Acadian tectonic evolution of South-Central New England. Am. J. Sci. 317, 34–94. https://doi.org/ 10.2475/01.2017.02.
- Millonig, L.J., Albert, R., Gerdes, A., Avigad, D., Dietsch, C., 2020. Exploring laser ablation U-Pb dating of regional metamorphic garnet – The Straits Schist, Connecticut, USA. Earth Planet. Sci. Lett. 552, 116589 https://doi.org/10.1016/j.epsl.2020.116589.
- Page, E.S., 1954. Continuous inspection schemes. Biometrika 41, 100–115. https://doi. org/10.2307/2333009.
- Pye, A.E., Hodges, K.V., Keller, C.B., Law, R.D., van Soest, M.C., Bhandari, B., McDonald, C.S., 2022. Prolonged slip on the South Tibetan detachment constrains tectonic models for synorogenic extension in the Central Himalaya. Tectonics 41, e2022TC007298. https://doi.org/10.1029/2022TC007298.
- Pyle, J.M., Spear, F.S., 2000. An empirical garnet (YAG) xenotime thermometer. Contrib. Mineral. Petrol. 138, 51–58. https://doi.org/10.1007/PL00007662.
- Pyle, J.M., Spear, F.S., Cheney, J.T., Layne, G., 2005. Monazite Ages in the Chesham Pond Nappe, SW New Hampshire, U.S.A.: implications for assembly of Central New England thrust sheets. Am. Mineral. 90, 592–606. https://doi.org/10.2138/ am.2005.1341.
- Pyle, J.M., Spear, F.S., Rudnick, R.L., McDonough, W.F., 2001. Monazite-xenotime-garnet equilibrium in metapelites and a new monazite-garnet thermometer. J. Petrol. 42, 2083–2107. https://doi.org/10.1093/petrology/42.11.2083.
- Regan, S.P., Walsh, G.J., Williams, M.L., Chiarenzelli, J.R., Toft, M., Mcaleer, R., 2019. Syn-collisional exhumation of hot middle crust in the Adirondack Mountains (New York, USA): implications for extensional orogenesis in the southern Grenville

- province. Geosphere 15, 1–22. https://doi.org/10.1130/GES02029.1/4694079/ges02029.pdf.
- Robinson, P., Tucker, R.D., Bradley, D., Berry IV, H.N., Osberg, P.H., 1998. Paleozoic orogens in New England, USA. GFF 120, 119–148. https://doi.org/10.1080/11035899801202119.
- Spear, F.S., 1993. Metamorphic Phase Equilibria and Pressure-Temperature-Time Paths, 1. Mineralogical Society of America, Mineralogical Society of America Monograph, Washington, D. C., p. 799
- Spear, F.S., Kohn, M.J., Cheney, J.T., 1999. P-T paths from anatectic pelites. Contrib. Mineral. Petrol. 134, 17–32. https://doi.org/10.1007/s004100050466.
- Spear, F.S., Pyle, J.M., 2002. Apatite, monazite, and xenotime in metamorphic rocks (in Phosphates; geochemical, geobiological, and materials importance) Reviews in Mineralogy and Geochemistry. Rev. Mineral. Geochem. 48, 293–335. https://doi. org/10.2138/rmg.2002.48.7.
- Spear, F.S., Pyle, J.M., 2010. Theoretical modeling of monazite growth in a low-Ca metapelite. Chem. Geol. 273, 111–119. https://doi.org/10.1016/j. chemsep.2010.02.016.
- Thomson, J.A., 2001. A counterclockwise P-T path for anatectic pelites, South-Central Massachusetts. Contrib. Mineral. Petrol. (141), 623–641. https://doi.org/10.1007/ s004100100265
- Tracy, R.J., Dietsch, C.W., 1982. High-temperature retrograde reactions in pelitic gneiss, central Massachusetts. Can. Mineral. 20, 425–437.
- Trayler, R.B., Schmitz, M.D., Cuitiño, J.I., Kohn, M.J., Bargo, M.S., Kay, R.F., Strömberg, C.A.E., Vizcaíno, S.F., 2019. An improved approach to age-modeling in deep time: implications for the Santa Cruz Formation, Argentina. In: GSA Bull., 132, pp. 233–244. https://doi.org/10.1130/B35203.1.
- Trayler, R.B., Meyers, S.R., Sageman, B.B., Schmitz, M.D., 2024. Bayesian integration of astrochronology and radioisotope geochronology. Geochronology 6, 107–123. https://doi.org/10.5194/gchron-6-107-2024.
- van de Schoot, R., et al., 2021. Bayesian statistics and modelling. Nat. Rev. Methods Prim. 1, 1. https://doi.org/10.1038/s43586-020-00001-2.
- Williams, M.L., Grover, T., Jercinovic, M.J., Regan, S.P., Pless, C.R., Suarez, K.A., 2019. Constraining the timing and character of crustal melting in the Adirondack Mountains using multi-scale compositional mapping and in-situ monazite geochronology. Am. Mineral. 104, 1585–1602. https://doi.org/10.2138/am-2019-6006
- Williams, M.L., Jercinovic, M.J., Hetherington, C.J., 2007. Microprobe monazite geochronology: understanding geologic processes by integrating composition and chronology. Annu. Rev. Earth. Planet. Sci. 35, 137–175. https://doi.org/10.1146/ annurev.earth.35.031306.140228.
- Williams, M.L., Jercinovic, M.J., Mahan, K.H., Dumond, G., 2017. Electron microprobe petrochronology. Rev. Mineral. Geochem. 83, 153–182. https://doi.org/10.2138/ rmg.2017.83.5.
- Yakymchuk, C., Clark, C., White, R.W., 2017. Phase relations, reaction sequences and petrochronology. Rev. Mineral. Geochem. 83, 13–53. https://doi.org/10.2138/ rmg.2017.83.2.